V. VOROBEL

Faculty of Mathematics and Physics, Charles University
(3, Ke Karlovu, 121 16 Praha 2, Czech Republic; e-mail: vit.vorobel@mff.cuni.cz)

LATEST RESULTS FROM NEUTRINO OSCILLATION EXPERIMENT DAYA BAY

The Daya Bay Reactor Neutrino Experiment was designed to measure θ_{13}, the smallest mixing angle in the three-neutrino mixing framework, with unprecedented precision. The experiment consists of eight identically designed detectors placed underground at different baselines from three pairs of nuclear reactors in South China. Since Dec. 2011, the experiment has been running stably for more than 7 years, and has collected the largest reactor antineutrino sample to date. Daya Bay greatly improved the precision on θ_{13} and made an independent measurement of the effective mass splitting in the electron antineutrino disappearance channel. Daya Bay also performed a number of other precise measurements such as a high-statistics determination of the absolute reactor antineutrino flux and the spectrum evolution, as well as a search for the sterile neutrino mixing, among others. The most recent results from Daya Bay are discussed in this paper, as well as the current status and future prospects of the experiment.

K e y w o r d s: neutrino oscillation, neutrino mixing, reactor, Daya Bay.

1. Daya Bay Neutrino Experiment

The Daya Bay Reactor Neutrino Experiment was designed to measure θ_{13}, the smallest mixing angle in the three-neutrino mixing framework, with unprecedented precision [1]. The experiment profits from a rare constellation of a nuclear power station complex situated near Hong Kong and adjacent mountains. The reactors serve as the source of neutrinos, while the mountains provide a sufficient overburden suppressing cosmic muons – the strongest background source (see Fig. 1). The Daya Bay and Ling Ao nuclear power plant (NPP) reactors (red circles) were situated on a narrow coastal shelf between the Daya Bay coastline and inland mountains.

At the time of the measurement, the facility consisted of six pressurized water reactors (PWRs). The electron antineutrinos are emitted in the beta-decay of fission fragments released in the chain reaction. The antineutrino flux and the energy spectrum is determined by the total thermal power of the reactor, the fraction of each fissile isotope in the fuel, the fission rate of each isotope, and the energy spectrum of neutrinos from each isotope. All the reactors have the same thermal power 2.9 GW$_{th}$ each and all together produced roughly 3.5×10^{21} $\tilde{\nu}_e$/s with ener-

gies up to 8 MeV making it one of the most intense $\tilde{\nu}_e$ sources on the Earth.

Two antineutrino detectors installed in each underground experimental hall near to the reactors (Hall 1 and Hall 2) measured the $\tilde{\nu}_e$ flux emitted by the reactors, while four detectors in the far experimental hall (Hall 3) measured a deficit in the $\tilde{\nu}_e$ flux due to oscillations in the location, where the neutrino oscillation effect is expected to be the strongest. Such configuration allows one to suppress the reactor-related uncertainty in the measured neutrino flux. The disappearance signal is most pronounced at the first oscillation minimum. Based on the existing accelerator and atmospheric neutrino oscillation measurements, this corresponded to the distance $L_f \approx 1.6$ km for the reactor $\tilde{\nu}_e$ with a mean energy of 4 MeV. The detectors were built and initially tested in a surface assembly building (SAB), transported to a liquid scintillator hall for the filling, and then installed in an experimental hall.

The detection of antineutrinos is based on the same principle as in the famous experiment of Reines and Cowan [2], who registered reactor antineutrinos in 1956. A sensitive part of the detector consists of a hydrogen-rich liquid scintillator doped with gadolinium (Reines and Cowan used Cd instead as the dopant). Antineutrino interacts via the inverse
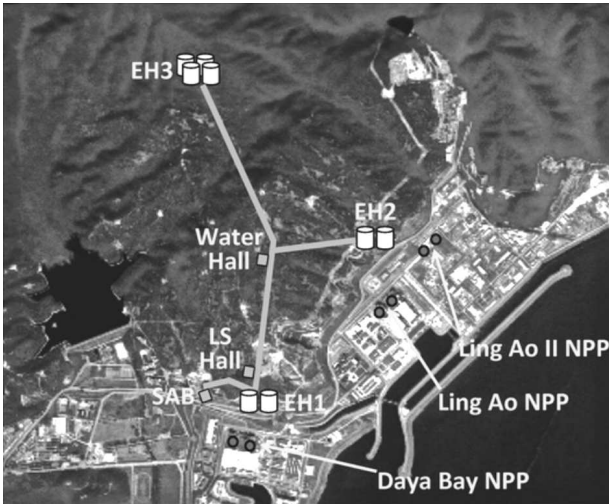
Fig. 1. Layout of the Daya Bay Neutrino Experiment

beta-decay (IBD)

$$\tilde{\nu}_e + p \to e^+ + n$$

with a proton (hydrogen) giving rise to a neutron and a positron. The positron deposits its kinetic energy to the scintillator, then annihilates on an electron, and generates two gamma rays, each 511 keV which together with the deposited positron kinetic energy cause a "prompt signal" within a few nanoseconds. The neutron is first moderated and then is captured on Gd typically 30 ns after the prompt signal. Consequently, a cascade of gamma quanta with a total energy of 8 MeV is emitted and generates a "delayed signal". The appearance of the two signals "prompt" and "delayed" is a signature of the antineutrino registration.

The Daya Bay antineutrino detector modules have an onion-like structure (see Fig. 2, left). The innermost volume is filled with 20 tons of the Gd-loaded liquid scintillator (GdLS) serving as the antineutrino target. The second layer – the gamma catcher – is filled with additional 20 tons of a normal liquid scintillator (LS) which can register most of the gamma energies from the neutron capture or positron annihilation. Neutrino interactions in the gamma catcher will not satisfy the trigger, since only the signal of the neutron-capture on Gd will trigger a neutrino event. The outer-most layer is normal mineral oil (MO) that shields the radiation from the PMT glass from entering the fiducial volume. The two inner vessels are fabricated of PMMA which is transparent for optical photons and chemically resistant against the used liquids, the outer-most 5 m by 5 m tank is made of a stainless steel and is equipped with 192 8-inch PMTs. Specular reflectors are located above and below the outer PMMA vessel to improve the light collection uniformity, while the vertical wall of the detector is black. Three automated calibration units are used to deploy radioactive sources (^{60}Co, ^{68}Ge, and ^{241}Am-^{13}C) and light-emitting diodes through narrow teflon-bellow penetrations into the GdLS and LS regions.

After the filling, the antineutrino detectors were installed in a 10 m deep water pool in each underground experimental hall, as shown in Fig. 2, right. The water shielded the detectors from γ-rays arising from the natural radioactivity and muon-induced neutrons, which were primarily emanated from the cavern rock walls. The pool was optically separated into two independent regions, the inner (IWS) and outer water shields (OWS). Both regions were instrumented with PMTs to detect the Cherenkov light produced by cosmogenic muons. A 4-layer resistive plate chamber (RPC) system was installed over the pool, which served in studies of muons and muon-induced backgrounds. The identification of muons which passed through the IWS, OWS, and RPC system enhanced the rejection of the background from neutrons generated by muon interactions in the immediate vicinity of the antineutrino detectors. Each detector (ADs, IWS, OWS) operated as an independently triggered system.

2. Results

2.1. Oscillation analysis based on n-Gd [3]

The presented results are from the analysis of data collected in the Daya Bay experiment with 6 detectors in 217 days (Dec/2011–Jul/2012), with 8 detectors in 1524 days (Oct/2012–Dec/2016), and with 7 detectors in 217 days (Jan/2017–Aug/2017). During 1958 days of operation, the Daya Bay experiment collected more than 3.5 millions inverse beta decays in the near halls and more than 0.5 million IBD have been detected in the far hall. The daily rate is ∼2500 IBD events in the near halls and ∼300 IBD in the far hall.

The distortion of the energy spectrum at the far hall relative to near halls was consistent with oscillations and allowed the measurement of $|\Delta m^2_{ee}|$. The
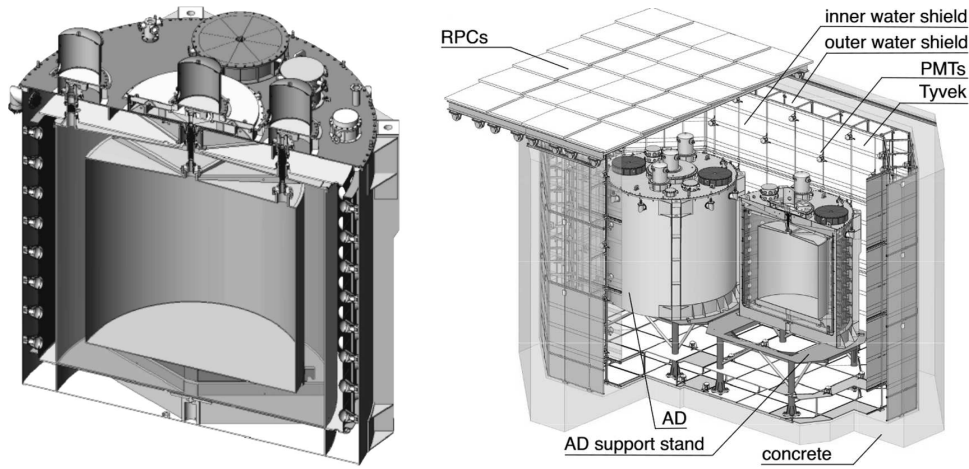
Fig. 2. Scheme of the antineutrino detector (AD) – left, and the near site detection view – right
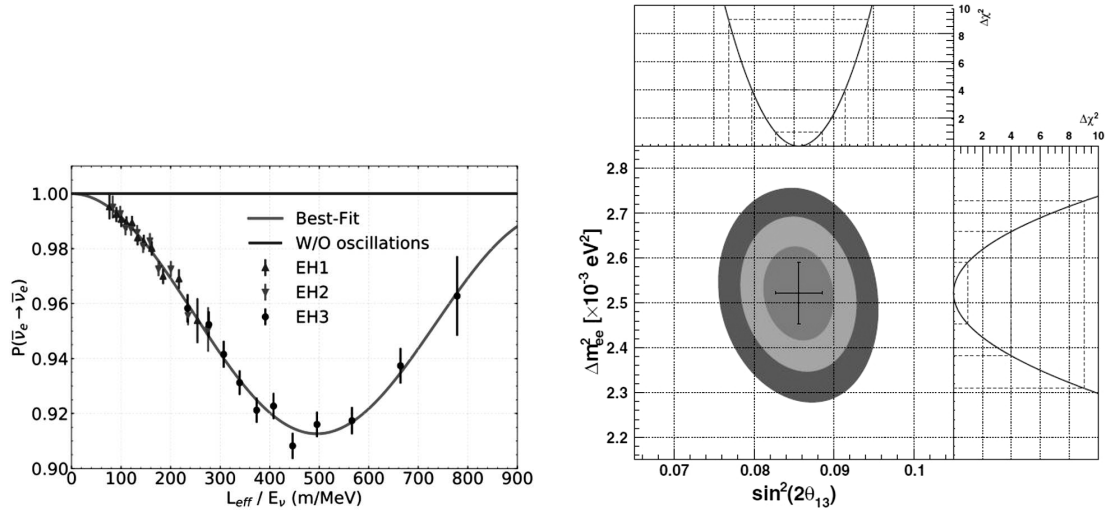

Fig. 3. Oscillation survival probability versus antineutrino proper time – left. The 68.3%, 95.5%, and 99.7% C.L. allowed regions for $\sin^2 2\theta_{13}$ and $|\Delta m_{ee}^2|$ – right

parameters of the three-flavor model in the best agreement with the observed rate and energy spectra were

$$\sin^2 2\theta_{13} = 0.0856 \pm 0.0029,$$

$$|\Delta m_{ee}^2| = [2.522^{+0.068}_{-0.070}] \times 10^{-3} \ \text{eV}^2,$$

$$\Delta m_{32}^2(NH) = +[2.471^{+0.068}_{-0.070}] \times 10^{-3} \ \text{eV}^2,$$

$$\Delta m_{32}^2(IH) = -[2.575^{+0.068}_{-0.070}] \times 10^{-3} \ \text{eV}^2.$$

The Δm_{32}^2 values were obtained under the assumptions of normal (NH) and inverted (IH) mass orderings.

Figure 3 – left, shows the observed electron survival probability as a function of the effective baseline L_{eff} divided by the average antineutrino energy $\langle E_\nu \rangle$. Almost one full oscillation disappearance and reappearance cycle was sampled, given the range of L/E_ν values which were measured.

The confidence intervals for Δm_{ee}^2 versus $\sin^2 2\theta_{13}$ are shown in Fig. 3 – right. The 1σ, 2σ, and 3σ 2-D confidence intervals are estimated using $\Delta\chi^2$ values of 2.30 (red), 6.18 (green), and 11.83 (blue) relative to the best fit. The upper panel provides the 1-D $\Delta\chi^2$ for $\sin^2 2\theta_{13}$ obtained by profiling $|\Delta m_{ee}^2|$ (blue line), and the dash lines mark the corresponding 1σ, 2σ,
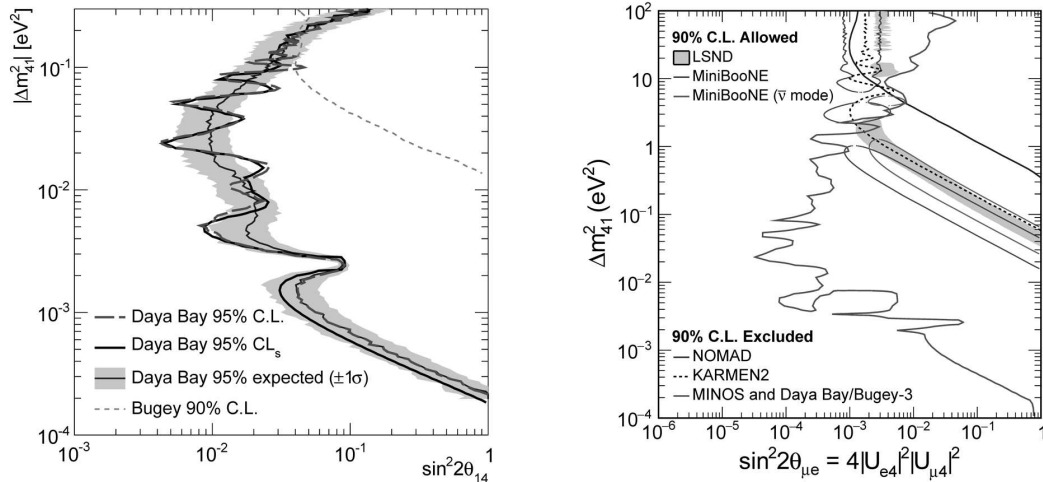
Fig. 4. Constraints for a sterile light neutrino provided by Daya Bay [13] – left, and the combined analysis of data from MINOS and Daya Bay/Bugey-3 [14] – right

and 3σ intervals. The right panel is the same, but for $|\Delta m_{ee}^2|$, with $\sin^2 2\theta_{13}$ profiled. The point marks the best estimates, and the error bars display their 1-D 1σ confidence intervals.

The Daya Bay results are compatible with the $\sin^2 2\theta_{13}$ results provided by other experiments: RENO [4], D-CHOOZ [5], T2K [6], MINOS [7], and $|\Delta m_{32}^2|$ values provided by RENO [4], T2K [6], MINOS [8], NOvA [9], Super-K [10], and IceCube [11]. While the accuracy of determination of $|\Delta m_{32}^2|$ is comparable with T2K and MINOS, the determination of $\sin^2 2\theta_{13}$ is more than twice more accurate than other results.

2.2. Oscillation analysis based on n-H [12]

The alternative analysis of data taken in 621 days and based on the events in which the neutron from IBD is captured on hydrogen results in

$$\sin^2 2\theta_{13} = 0.071 \pm 0.011.$$

The combination of the n-H and n-Gd results from 1230 days data gives the 8% improvement in precision:

$$\sin^2 2\theta_{13} = 0.082 \pm 0.004.$$

2.3. Search for Light Sterile Neutrino

The large statistics collected with the full configuration of eight detectors in the Daya Bay experiment allowed a new precise analysis with aim to search

for a light sterile neutrino [13]. A relative comparison of the rate and energy spectrum of reactor antineutrinos in the three experimental halls yields no evidence of the sterile neutrino mixing in the $2 \times 10^{-4} < |\Delta m_{41}^2| < 0.3$ eV^2 mass range. The resulting limits on $\sin^2 2\theta_{14}$ shown in Fig. 4 – left, constitute the most stringent constraints to date in the $|\Delta m_{41}^2| < 0.2$ eV^2 region.

Searches for a light sterile neutrino have been independently performed by the MINOS and Daya Bay experiments using the muon (anti)neutrino and electron antineutrino disappearance channels, respectively. Results from both experiments are combined with those from the Bugey-3 reactor neutrino experiment to constrain oscillations into light sterile neutrinos [14]. The three experiments are sensitive to complementary regions of the parameter space, enabling the combined analysis to probe the regions allowed by the LSND and MiniBooNE experiments in a minimally extended four-neutrino flavor framework. Stringent limits on $\sin^2 2\theta_{\mu e}$ are set over six orders of magnitude in the sterile mass-squared splitting Δm_{41}^2. The sterile-neutrino mixing phase space allowed by the LSND and MiniBooNE experiments is excluded for $\Delta m_{41}^2 < 0.8$ eV^2 at 95% CLs, see Fig. 4 – right.

2.4. Reactor antineutrino flux and spectrum anomalies [15]

Data collected in 1230 days were used to measure the IBD yield in four near detectors. The new av-
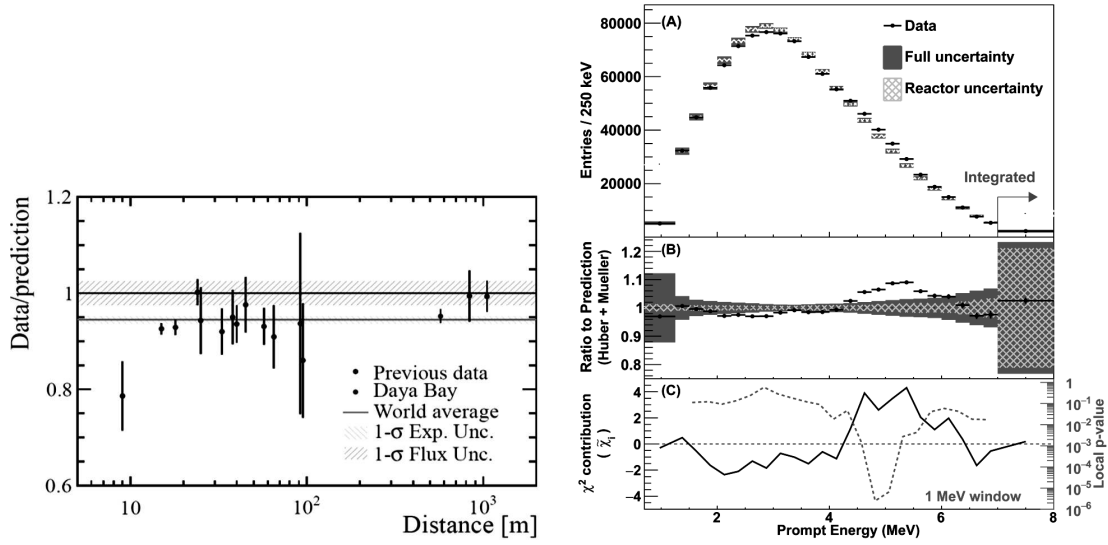
Fig. 5. Ratio of the measured antineutrino yield to the Huber–Vogel theoretical prediction vs. the distance from detector to detector – left. Comparison of the predicted and measured prompt energy spectra – right
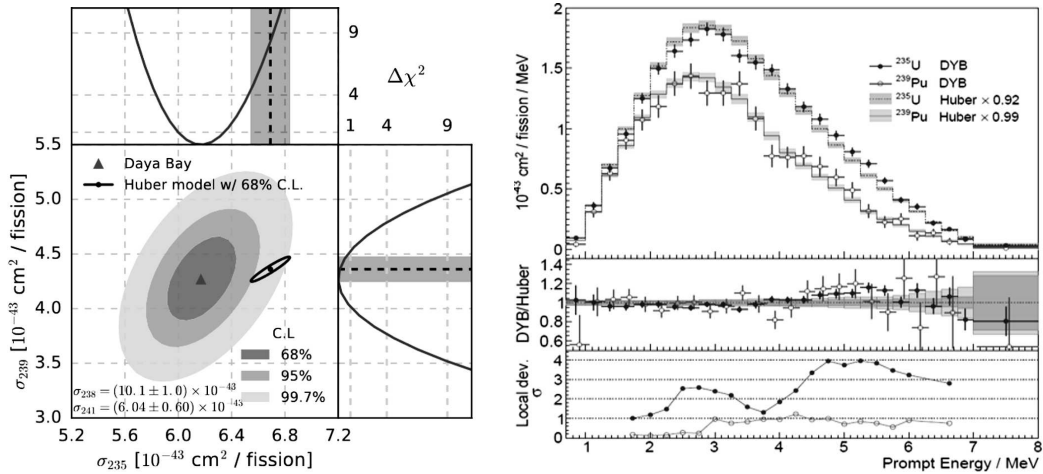

Fig. 6. Combined measurement of ^{235}U and ^{239}Pu IBD yields per fission σ_{235} and σ_{239} – left. Decomposition of the reactor anti-neutrino spectrum into two dominant contributions from ^{235}U and ^{239}Pu

erage IBD yield is determined to be $(5.91 \pm 0.09) \times \times 10^{-43}$ cm^2/fission, and the updated ratio of measured to predicted flux was found to be $0.952 \pm 0.014 \pm 0.023$ and $1.001 \pm 0.015 \pm 0.027$ for the Huber + Mueller and ILL + Vogel models, respectively, where the first and second uncertainties are experimental and theoretical model uncertainties, respectively. The tension with respect to the theoretical predictions is consistent with other experiments, see Fig. 5 – left. In particular, an excess of events in the region of 4–6 MeV was found in the measured spec-

trum, with a local significance of 4.4σ, see Fig. 5 – right.

2.5. Evolution of the reactor antineutrino flux and spectrum [16]

The data taken by the detectors in two near halls in 1230 days spanning multiple fuel cycles for each of the reactors were used for the investigation of the evolution of the antineutrino flux and spectrum. Weakly effective fission fractions values corresponding to the fission isotopes ^{235}U, ^{238}U, ^{239}Pu, and ^{241}Pu for each

detector were calculated using thermal power and fission fraction data for each core, which were provided by the power plant.

A decrease of the total IBD yield/fission with increase of the effective fission fraction F_{239} of ^{239}Pu (larger fuel burn-up) was clearly observed. Individual yields σ_{235} and σ_{239} from the main flux contributors ^{235}U and ^{239}Pu, respectively, were fitted, see Fig. 6 – left. The discrepancy in a variation of the antineutrino flux from ^{235}U with respect to the reactor fuel composition model prediction suggests a 7.8% overestimation of the predicted antineutrino flux from ^{235}U and indicates that this isotope could be the primary contributor to the reactor antineutrino anomaly.

2.6. Reactor antineutrino spectrum decomposition [17]

The analysis of 3.5 milions of events taken during 1958 days in four near antineutrino detectors allows the partial decomposition of the antineutrino spectra – see Fig. 6 – right. The IBD yields and prompt energy spectra of ^{235}U and ^{239}Pu are obtained using the evolution of the prompt spectrum as a function of the fission fractions. The analysis confirms the discrepancy between the measured spectrum shape and the prediction. The deviation is 5.3σ and 6.3σ in the energy interval 0.7–8 MeV and in a local energy interval of 4–6 MeV, respectively.

The comparison of the measured and predicted ^{235}U and ^{239}Pu IBD yields preferes an incorrect prediction of the ^{235}U flux as the primary source of the reactor antineutrino rate anomaly. The discrepancy in the spectral shape for ^{235}U suggests the incorrect spectral shape prediction for the ^{235}U spectrum. However, no such conclusion can be drawn for the ^{239}Pu spectrum due to a larger uncertainty.

1. F.P. An *et al.* (Daya Bay Collaboration). Observation of electron-antineutrino disappearance at daya bay. *Phys. Rev. Lett.* **108**, 171803 (2012).

2. C.L. Cowan, F. Reines, F.B. Harrison, H.W. Kruse, A.D. McGuire. Detection of the free neutrino: A confirmation. *Science* **124**, 103 (1956).

3. D. Adey *et al.* (Daya Bay Collaboration). Measurement of the electron antineutrino oscillation with 1958 days of operation at daya bay. *Phys. Rev. Lett.* **121**, 241805 (2018).

4. J.H. Choi *et al.* (RENO Collaboration). Observation of energy and baseline dependent reactor antineutrino disappearance in the RENO experiment. *Phys. Rev. Lett.* **116**, 211801 (2016) (arXiv:1511.05849 [hep-ex]).

5. M. Ishitsuka. (Double Chooz Collaboration). First results with two detectors from Double Chooz. In: *Proc., 51st Rencontres de Moriond on Electroweak Interactions and Unified Theories : La Thuile, Italy, March 12–19* (2016), p. 157.

6. K. Iwamoto. (T2K Collaboration). Recent results from T2K and future prospects. *38th Int. Conf. on High Energy Physics* (2016), PoS(ICHEP2016)517.

7. P. Adamson *et al.* (MINOS Collaboration). Electron neutrino and antineutrino appearance in the full MINOS data sample. *Phys. Rev. Lett.* **110**, 171801 (2013).

8. J. Evans. (MINOS and MINOS+ Collaborations). New results from MINOS and MINOS+. *27th Int. Conf. on Neutrino Physics and Astrophysics, London, UK, July 4–9, 2016. J. Phys.: Conf. Ser.* **888**, 012017 (2017).

9. P. Vahle. (NOvA Collaboration). New results from NOvA. *27th Int. Conf. on Neutrino Physics and Astrophysics, London, UK, July 4–9, 2016. J. Phys.: Conf. Ser.* **888**, 012003 (2017).

10. S. Moriyama. (Super-Kamiokande Collaboration). New atmospheric and solar results from Super-Kamiokande. *27th Int. Conf. on Neutrino Physics and Astrophysics, London, UK, July 4–9, 2016. J. Phys.: Conf. Ser.* **888**, No. 1, 012005 (2017).

11. J. Koskinen. (Ice Cube Collaboration). Atmospheric neutrino results from IceCube-DeepCore and plans for PINGU. *27th Int. Conf. on Neutrino Physics and Astrophysics, London, UK, July 4–9, 2016. J. Phys.: Conf. Ser.* **888**, No. 1, 012023 (2017).

12. F.P. An *et al.* (Daya Bay Collaboration). New measurement of θ_{13} via neutron capture on hydrogen at Daya Bay. *Phys. Rev. D* **93**, 072011 (2016).

13. F.P. An *et al.* (Daya Bay Collaboration). Improved search for a light sterile neutrino with the full configuration of the Daya Bay experiment. *Phys. Rev. Lett.* **117**, No. 15, 151802 (2016).

14. F.P. An *et al.* (Daya Bay Collaboration, MINOS Collaboration). Limits on active to sterile neutrino oscillations from disappearance searches in the MINOS, Daya Bay, and Bugey-3 experiments. *Phys. Rev. Lett.* **117**, No. 15, 151801 (2016).

15. D. Adey. *et al.* (Daya Bay Collaboration). Improved measurement of the reactor antineutrino flux at Daya Bay. arXiv:1808.10836 (2018).

16. F.P. An *et al.* (Daya Bay Collaboration). Evolution of the reactor antineutrino flux and spectrum at Daya Bay. arXiv:1704.01082 (2017).

17. D. Adey *et al.* (Daya Bay Collaboration). Measurement of individual antineutrino spectra from ^{235}U and ^{239}Pu at Daya Bay. arXiv:1904.07812 (2019).

В. Воробел
від імені Колаборації Daya Bay

НОВІТНІ РЕЗУЛЬТАТИ
З ЕКСПЕРИМЕНТУ НЕЙТРИННИХ
ОСЦИЛЯЦІЙ DAYA BAY

Р е з ю м е

Експеримент з реакторними нейтрино DAYA BAY задумано для вимірювання Θ_{13} – найменшого кута в рамках тринейтринного змішування – з безпрецедентною точністю. Експериментальна система складається з восьми однакових детекторів, розміщених під землею на різних базових відстанях від трьох пар ядерних реакторів Південного Китаю. Починаючи від 2011 року, експериментальна система працює стабільно впродовж більш ніж 7 років та накопичила найбільше як на сьогодні даних про реакторні антинейтрино. DAYA BAY значно покращив точність Θ_{13} і виконав незалежні вимірювання ефективного розщеплення мас в каналі зникнення електронного нейтрино. DAYA BAY провів також інші точні експерименти, такі як вимірювання з високою точністю абсолютного потоку реакторних нейтрино і їхнього спектра, а також пошук змішування стерильних нейтрино. В даній роботі обговорюються новітні результати з DAYA BAY, а також сучасний стан та перспективи експерименту.